2

Transparent ZnO Electrode for Liquid Crystal Displays

Naoki Yamamoto, Hisao Makino and Tetsuya Yamamoto
Research Institute, Kochi University of Technology
Japan

1. Introduction

Recently, the scarcity and toxicity of indium, a major constituent element of ITO, has become a concern. Indium is a rare element that ranks 61st in abundance in the Earth's crust (Kempthorne & Myers 2007). In addition, the major amounts of indium consumed by the industries produceing the electronic devices such as liquid crystal displays (LCDs), touch-screens and solar cell systems are supplied by only a few countries. Furthermore, indium has also been suspected to induce lung disease, and particularly indium-related pulmonary fibrosis should be paid attention (Homma et al., 2005).
Transparent conductive oxides have become the focus of attention as a substitute material for ITO currently used for optically transparent electrodes in electronic devices. In particular, transparent conductive ZnO films are expected to be suitable materials to achieve such purposes because, in contrast with indium as a major constituent element of ITO, Zn is an element that the human body requires and is a component of some marketed beverages, in addition to having being used for years in cosmetics and as a vulcanization accelerator for rubber products such as tires. Furthermore, conductive and transparent ZnO films have low electrical resistance and high optical transmittance comparable with those of ITO films reported by some authors (Wakeham et al., 2009; Shin et al., 1999). We have developed the technology to form transparent conductive ZnO films with low resistance (2.4 μΩ m for a 100 nm thick film (Yamada, et al., 2007)), optical transmittance exceeding 95% (film-only transmittance without that of the glass substrate) and high heat-resistance (thermally stable until 300-450 °C (Yamamoto, N. et al., 2010)). The technology of transparent conductive ZnO films applied as alternatives to ITO electrodes for LCD panels is described in this chapter.

2. Preparation of transparent and conductive ZnO film

Ga-doped ZnO (GZO) and Al-doped (AZO) films have been widely studied as the most promising transparent conductive films as alternatives to ITO films used in electronics devices such as LCDs, LEDs and solar cells.

2.1 Magnetron sputtering system

Conventional magnetron sputtering systems, planar- and cylindrical-types (Carousel-type), were used to form transparent ZnO thin films. A schematic diagram of the cylindrical-type magnetron sputtering system is shown in Fig. 1 (a). In the cylindrical-type magnetron

sputtering system, a drum with samples set on its surface is rotated concentrically in the chamber with the sputtering target set on the inside wall. A film can be formed by sputtering with dc power (noted as dc MS) and radio frequency power combined with dc power (noted as rf+dc MS) applied to the sputtering target.

2.2 Reactive plasma deposition system

Figure 1 (b) shows a schematic diagram of the reactive plasma deposition system (RPD) (Yamamoto, T. et al., 2008)., which is a type of ion-plating method. An Ar plasma stream is generated by a pressure gradient arc plasma source (Uramoto gun) at the cathode is introduced by control of the electric and the magnetic field to the evaporation source tablet inset in the hearth at the anode. The particles evaporated from the source are deposited onto the substrate set on the tray traveling in front of the heater.

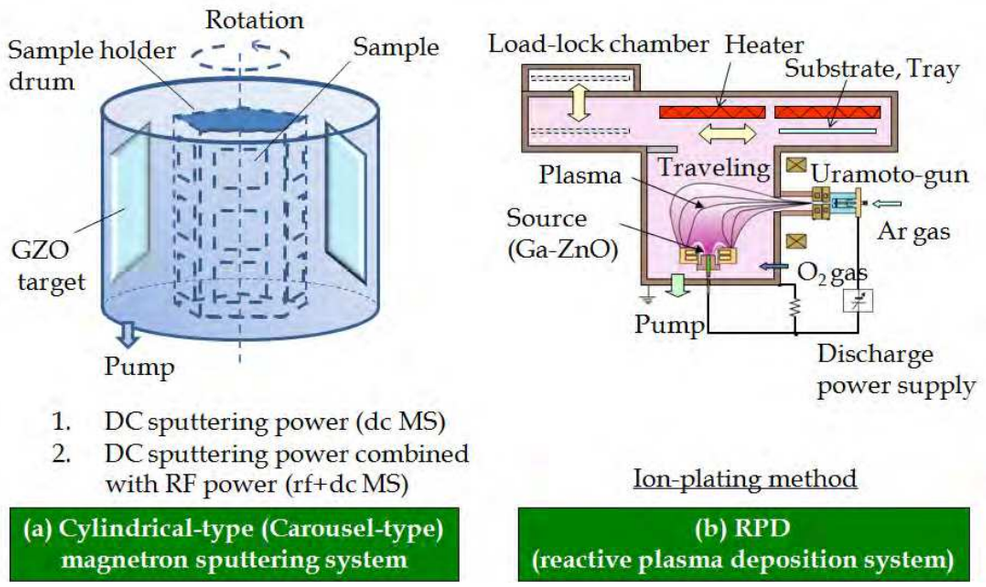

Fig. 1. Schematic diagrams of the deposition systems for the transparent conductive ZnO films.

The specifications for the formation of conductive transparent ZnO film using the magnetron sputtering systems and the RPD system are summarized in Table 1

	Magnetron Sputtering (MS)		RPD
	dc MS	rf+dc MS	
Ga_2O_3/Al_2O_3 content in ZnO source (wt%)	Ga_2O_3: 3.0 - 6.0		Ga_2O_3: 3.0 - 5.0
	Al_2O_3: 2.0 - 5.0		
Power (kW)	0.1 - 2.0	rf: 0.1 - 1.5, dc: 0.1 - 1.5 rf/dc = 0.5 - 2.0	discharge current: 140 - 150 (A)
Operation pressure (Pa)	0.1 - 0.8	0.1 - 0.8	0.4 - 0.6
Operation temperature (°C)	25 - 350	25 - 350	25 - 250

Table 1. Specifications for the formation of GZO or AZO films (Yamamoto. N. et al., 2011a & 2011c).

An Ar plasma stream is generated by a pressure gradient arc plasma source (Uramoto gun) at the cathode is introduced by control of the electric and the magnetic field to the evaporation source tablet inset in the hearth at the anode. The particles evaporated from the source are deposited onto the substrate set on the tray traveling in front of the heater.
The specifications for the formation of conductive transparent ZnO film using the magnetron sputtering systems and the RPD system are summarized in Table 1

3. Basic characteristics of transparent conductive ZnO film

The fundamental characteristics of transparent conductive ZnO films for application to LCD panels are discussed in this section.

3.1 Crystalline structure of transparent conductive ZnO film

X-ray diffraction (XRD; ATX-G, Rigaku) and transmission electron microscopy (TEM; H-9000UHR; Hitachi High-technologies Co.) were applied for analysis of the crystalline structures of transparent conductive ZnO films.
The crystalline structures and orientations of the GZO films were analyzed using both out-of-plane XRD (widely used X-ray diffraction analysis) and in-plane XRD (grazing-incidence wave-dispersive X-ray analysis (Ofuji et al., 2002)). For measurement using the in-plane XRD technique, a Cu Kα X-ray beam with a wavelength of 0.154184 nm was irradiated at a low angle of incidence to the surface of the sample (0.35°). The incident angle is close to the total reflection angle of X-ray for ZnO.
XRD patterns obtained from the GZO films deposited by dc MS, rf+dc MS or RPD were almost identical and had the wurtzite crystalline structure, as with the ZnO films. A typical XRD pattern obtained from a GZO film is shown in Fig. 2.
The in-plane XRD diffraction pattern shows that no diffraction peaks from the ZnO(00x) crystal planes were evident (Fig. 2(a)). In contrast, the out-of plane XRD pattern shows only the (002) and (004) diffraction peaks of the GZO film (Fig. 2(b)).
The appearance of these diffraction peaks clarified that (1) the GZO polycrystalline film consists of the wurtzite structure. (2) the *c*-axes of the wurtzite structure coincides with the direction normal to the GZO film surface, and (3) the *a*-axes of the wurtzite cell structure coincides with the direction in the plane of the film. The TEM image in Fig. 3(a) and the cell structure shown in Fig. 3(b) explains the structure. Columnar grains comprise the interior of the polycrystalline GZO films (Yamamoto. N. et al., 2008). Such crystalline structures also appeared in films formed in the temperature range of 150-250 °C using dc MS, rf+dc MS and RPD.
The lattice constants for the *c*- and *a*-axes, and the volume of the wurtzite crystalline unit cell in 100 nm thick GZO films prepared at 180 °C by dc MS, rf+dc MS and RPD were derived using the XRD peaks diffracted from the (00x) and (x00) crystalline planes and are compared in Fig. 4 (Yamamoto, N. et al., 2010). The lattice constants of the GZO films prepared by RPD were shorter than those of the films formed by magnetron sputtering (Fig. 4(a)). The *c*-axis of the rf+dc MS film was especially expanded toward the direction normal to the surface of the substrate compared with the other films. The *a*-axis was also expanded toward in the direction of the plane of the film. As a result, the cell volume of the wurtzite structure in the films prepared by rf+dc MS were larger than those formed by dc MS and RPD, as shown in Fig. 4 (b).

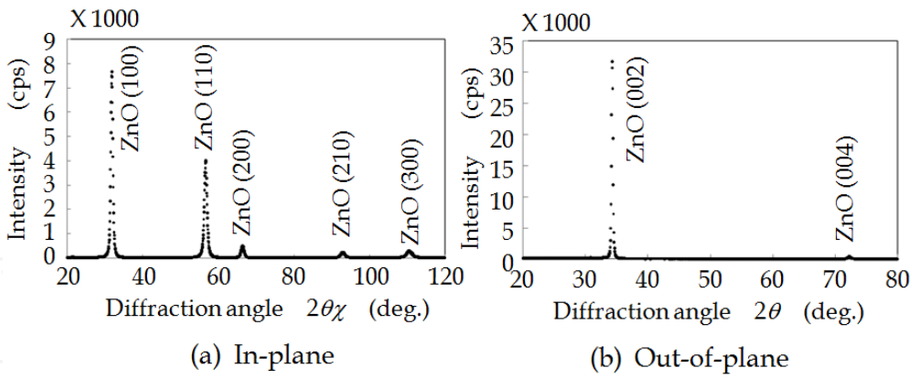

Fig. 2. Typical XRD profile of a 150 nm thick GZO film prepared at 180 °C using dc MS.

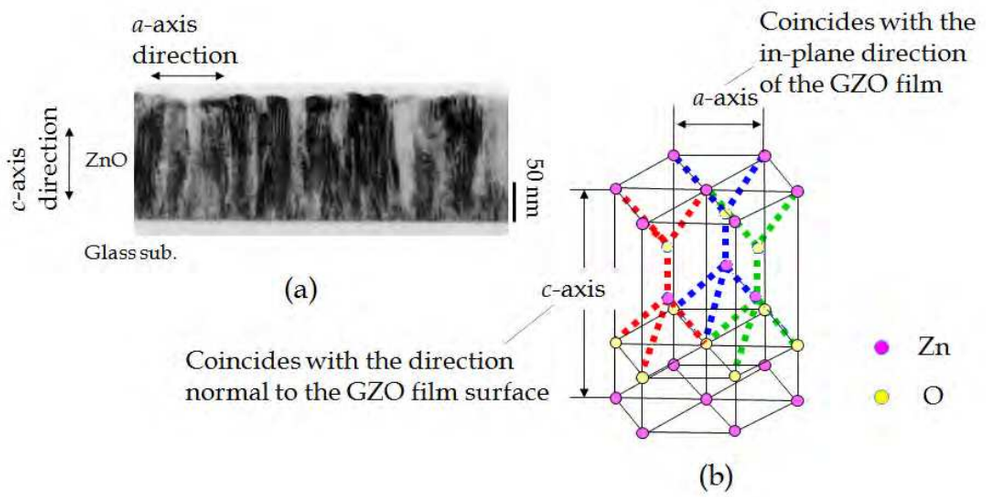

Fig. 3. (a) Cross-sectional TEM image of GZO film formed by dc MS and (b) the wurtzite cell structure.

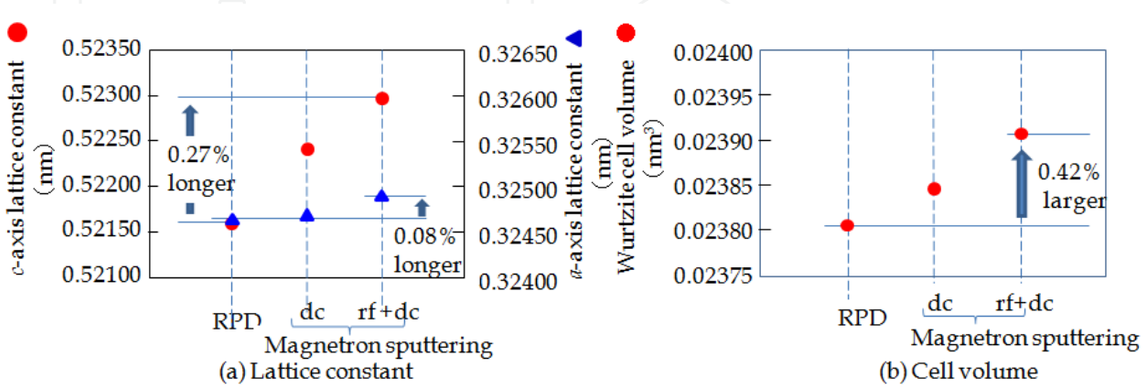

Fig. 4. Comparison of the *a*-axis, *c*-axis lattice constants and the unit cell volumes in crystalline ZnO-based wurtzite structures of films prepared using dc MS, rf+dc MS and RPD (Yamamoto,N. et al 2010).

3.2 Resistance of transparent conductive ZnO film

The resistivity of the film is one of the most important characteristics required for application of alternative transparent electrodes to ITO used in LCDs. The resistivity of ITO transparent films is in the range of 1.3–3.8 μΩm (Wakeham, et al.. 2009; Shin et al., 1999). Therefore, transparent conductive ZnO films as an alternative must have a resistivity of less than ca. 3.8 μΩm.

In the case of thin films, the resistivity is generally derived from the carrier-flow in the plane of the films. The resistivities of even metal films increase with the decrease in film thickness, especially less than ca. 100 nm. Such a phenomenon is caused by the increase in the frequency of collisions or scattering with the carrier–flow and the film surface, the interface with the substrate and irregular crystalline structures in the region of the substrate. The resistivity of the GZO film also shows a similar dependency on the film thickness, as shown in Fig. 5(a).

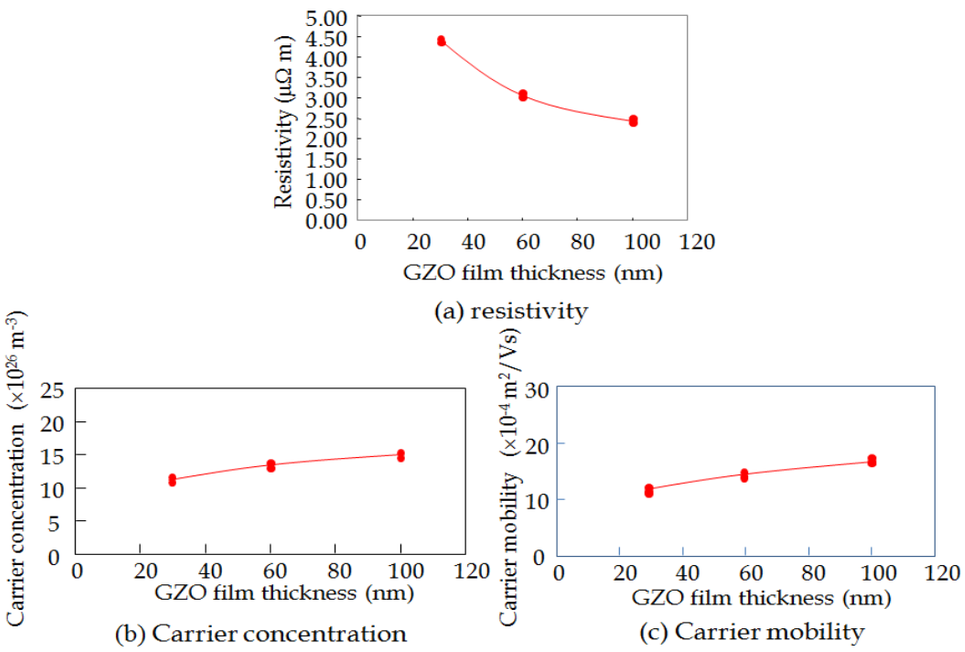

Fig. 5. Electrical characteristics of GZO film as a function of the film thickness.

As the film thickness decreases, the carrier mobility and concentration in the film decreases, as shown in Figs. 5(b) and (c). The data in Fig. 5 was obtained from GZO films prepared using RPD at 180 °C. The electrical characteristics of transparent conductive ZnO films formed by the magnetron sputtering showed similar dependencies on the film thickness, although the values were significantly affected by the formation conditions, i.e., type of dopant and its concentration, the deposition equipment, temperature, pressure and the electrical power supplied to the source during deposition.

Figure 6 shows a comparison of the resistivities of GZO and AZO films formed with an Ar sputtering pressure of 0.66 Pa at room temperature or at 180 °C using the conventional planar magnetron sputtering system. The ZnO sputtering target materials for the deposition of GZO or AZO contained 4 wt% Ga_2O_3 or 2 wt% Al_2O_3, respectively. The total sputtering power used in both cases of dc MS and rf+dc MS was set to 200 W.

The resistivities of the AZO films were 1.5 times or more higher than those of the GZO films. The resistivities of the films formed by rf+dc MS were lower than those of films formed by dc MS (Yamamoto, N. et al., 2011a & 2011c). However, this relationship does not correspond to the lattice constants and cell volumes of the wurtzite structures of the GZO films formed by rf+dc MS, which were larger than those of the films formed by dc MS, as shown in Figs. 4(a) and (b). It is generally considered that the probability of carrier hopping among atoms decreases with distance from each atomic site, and as a result, the resistivity of the film decreases with the length of the lattice constant. The reason for the contradiction between the resistivity and the lattice constant (length) is yet to be clarified.

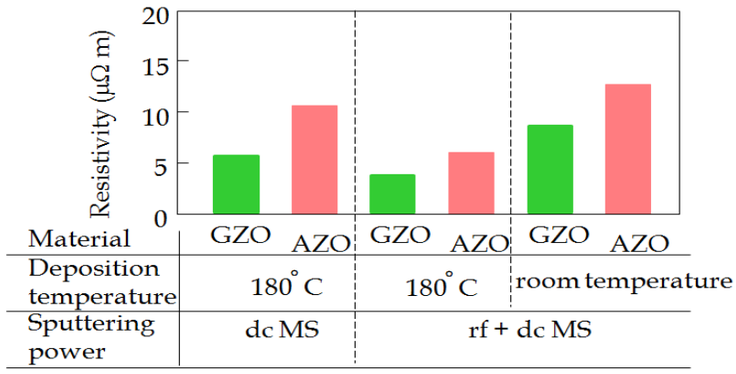

Fig. 6. Comparison of resistivity for ca. 150 nm thick transparent ZnO films formed by dc MS and rf+dc MS

3.3 Visible light transmittance of transparent conductive ZnO film

Alternative materials to the ITO electrodes used for LCDs are required to have transmittance for visible light comparable with that of ITO films. The optical transmittance of the films was analyzed using an optical spectrophotometer (U-4100 UV-Visible-NIR spectrophotometer, Hitachi High-tech. Co. Ltd.). The transmittance of the GZO films in the wavelength range of ultraviolet (UV) to near-infrared (NIR) is shown in Fig. 7(a) The transmittance values presented in this section include the transmittance of the glass substrate. The absorption edges in the spectra are shifted slightly to the shorter side from the wavelength (ca. 370 nm) corresponding to the bandgap of undoped-ZnO according to the Burstein–Moss effect (Moss 1980).

On the other hand, the transmittance in the NIR region was significantly reduced from an increase of reflectance due to the plasma resonance of electron gas in the conduction band in the films with highly density carriers (electrons) of 8×10^{26} to 1.5×10^{27} m^{-3} (Jin et al., 1988; Dong & Fang 2007). The transmittance spectra in the wavelength region of visible light are scaled up in Fig. 7(b). Undulations in the transmittance spectra as a function of wavelength appeared due to optical interference phenomena caused at the surface and at the interface with the glass substrate because the dependency of the 110 nm thick sample on the wavelength differed from those of the ca. 150 nm thick samples. The maximum, minimum and average transmittance of each sample in the range of 400–800 nm were 90.5 – 91.4, 73.1 – 86.4, 87.2 – 87.8, respectively.

The transmittance of a 150 nm thick GZO film formed at 200 °C by conventional dc MS on a 1.1 mm thick Corning #1737 glass substrate was compared with polycrystalline and amorphous ITO films with ca. 150nm thickness formed using a similar sputtering system,

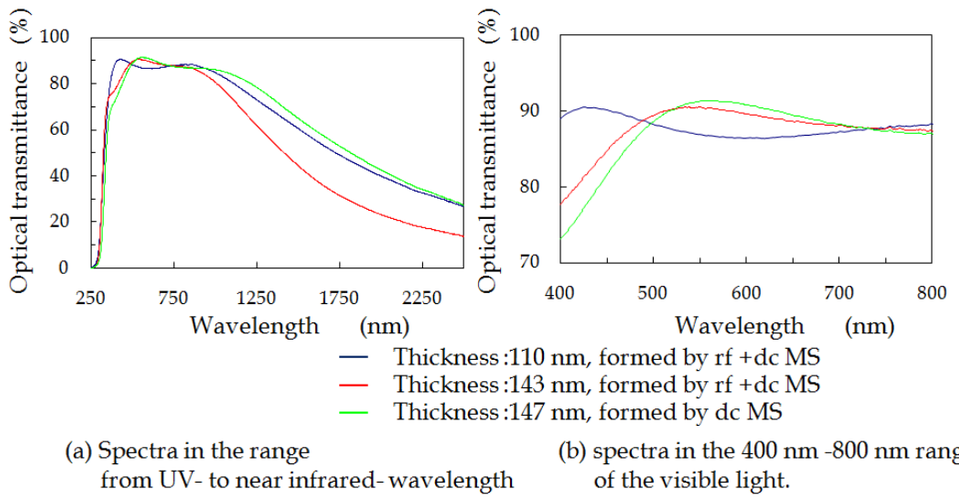

Fig. 7. Comparison of optical transmittance of films formed at 180 °C using rf+dc MS and dc MS on 0.7 mm thick Corning #1737 glass substrates.

and the results are shown in Fig. 8 (Yamamoto, N. et al., 2011a & 2011c). The exact deposition conditions is proprietary and therefore limited to announcement by Geomatec Co., Ltd. Japan. The amorphous and polycrystalline ITO films were formed at approximately 50-70 and 250-300 °C, respectively. The optical transmittance of the GZO film surpassed those of the ITO films in the entire wavelength range of visible light. Visible light in the range of 400-550 nm was transmitted through the GZO film with 2-7% higher transmittance than those of the ITO films.

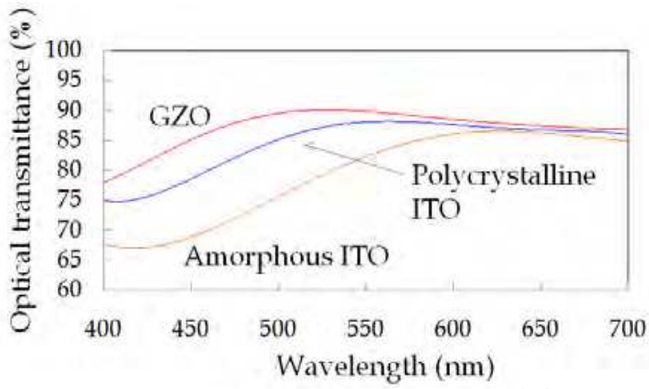

Fig. 8. Comparison of the optical transmittance of transparent GZO and ITO films.

3.4 Residual stress in transparent conductive ZnO film

The development of transparent conductive films that are resistant against external forces and forces induced by thermal processes (maximum temperature: ca. 250 °C) during LCD fabrication requires investigation of the fundamental mechanical characteristics of the films, such as residual stress, thermal stress, strain, Young's modulus, coefficient of thermal expansion, adhesive force and creep. In this section, the residual stress of GZO films is discussed. The conventional optical lever method was applied for residual stress analysis using a HeNe-laser beam at 633 nm (F2300, Flexus Co.). The Si wafer substrate was used as a

reflector for the laser beam. The substrate with film was placed on the three projections attached with an equilateral-triangular layout on the surface of the heater plate. The radius of curvature of the Si wafer was measured by detecting the reflected beam. The stress in the film was then derived using the curvature radius, the linear coefficient of thermal expansion (3.34×10^{-6} K^{-1}) and the Young's modulus (160 GPa) of the Si substrate (Wortman & Evans 1965).

The wafer was heated from 25 to 500 °C and subsequently cooled to 25 °C for heat-cycle testing of the film, and the curvature radius of the Si wafer was measured *in situ* during testing. The residual stresses of all the as-deposited films were artificially set to compressive, according to the controlled deposition processing factors. The residual stress in a film is dependent on the degree of energetic particle bombardment, that is, energy striking the condensing film during deposition by magnetron sputtering or RPD with plasma discharge discharge (Thornton, & Hoffman, 1977; Yamamoto, N. et al., 1986).

The residual stress properties of the films were clarified by applying heat-cycle testing. Heat-cycle testings was applied twice to each sample. The samples were heated at a rate of 2.8 °C/min until thermal equilibrium (thermally quasi-static condition) and *in situ* measurements of residual stresses in the films were conducted during heat-cycle testing.

The residual stresses of the films formed at 180 °C using rf+dc MS, dc MS and RPD had following similar behaviors, as shown in Fig. 9 (Yamamoto, N. et al., 2008 & 2010). (I) the residual stress in the films was significantly reduced in the range from 200 to 400 °C during the first heating-up process (step 1); there was an increasing tendency toward strongly compressive residual stress, which changed abruptly to the tensile direction upon heating. This critical temperature of change is dependent on the deposition method of the films. (II) the stress decreased monotonically with cooling from 500 °C (step 2), and (III) the dependence of the stress in each film on the temperature during the second heat-cycle (steps (3) and (4)) almost coincided with that in step (2). These phenomena present evidence that the extrinsic stress components in each film are removed by annealing during the first heating step to 500 °C, and the resulting stress is composed of only thermal stress, i.e., intrinsic stress. The thermal stress is caused by the difference in the linear coefficient of thermal expansion between the GZO film and the Si substrate.

On comparatively thicker GZO films (ca. 500 nm in Fig. 9) formed by dc MS and RPD, the temperature dependencies in step (1) were closer to those in the second cycle testing. The main component of internal stress in such thick films was thermal stress (intrinsic stress), even before heat-cycle testing of the as-deposited film. The GZO films approached the ideal crystalline structure as the thickness increased. The overall temperature dependency change of the residual stresses according with the film thickness corresponds approximately with the increase in crystalline irregularity with the distance from the interface to the substrate. On the other hand, the GZO film thicker than 500 nm formed by rf+dc MS did not provide the same stress behavior in step (1) in the GZO closed to those in steps (2) to (4). High strain or irregular crystalline structures were present until a far distance from the substrate surface of the film.

4. Fabrication of LCD panels with transparent ZnO electrodes on RGB color filters

4.1 Intrinsic weakness of transparent conductive ZnO film in the LCD manufacturing environment

The fundamental properties of GZO films as an alternative to ITO transparent electrodes have been clarified with experimental results. However, the properties required for

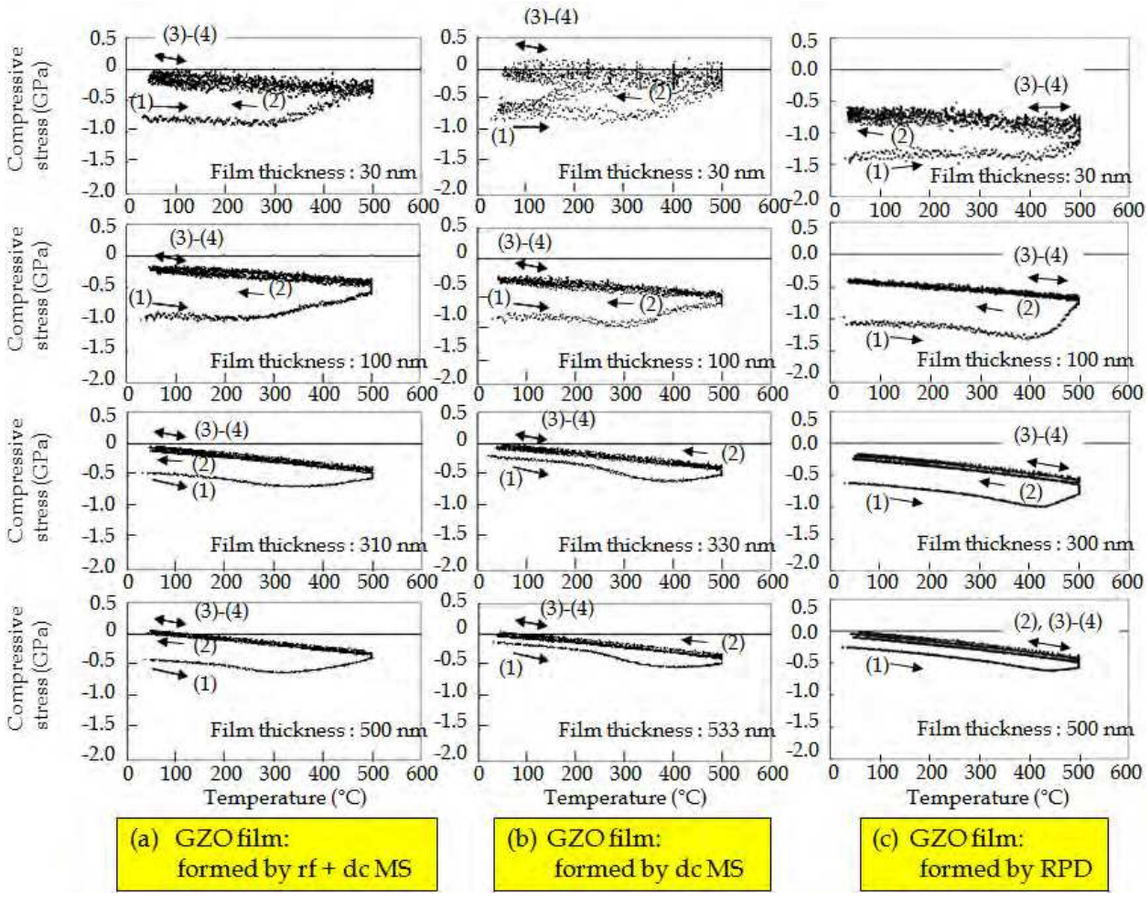

Fig. 9. Comparison of residual stress behavior during heat-cycle testing from room temperature to 500°C in an Ar atmosphere.

application in the production of the LCDs have not yet been discussed thoroughly. ZnO or materials based on ZnO have significant impediments to LCD applications. Such materials have amphoteric properties, so that their films have the extremely low tolerability to the various process conditions and environments used for manufacturing and operating LCD panels, i.e., acidic, basic and highly humid environments. Furthermore, Zn atoms are easily volatilized from materials by heating processes at relatively low temperature such as 300-400 °C. Transparent electrode films are required to endure manufacturing processes at ca. 250 °C for the fabrication of LCDs. A diagrammatic cross-sectional illustration of an LCD is shown in Fig. 10.

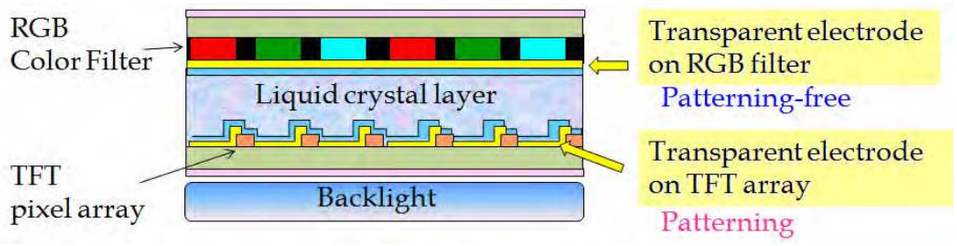

Fig. 10. Schematic cross-sectional view of an LCD.

The transparent conductive films on the RGB color filter is generally used without patterning. On the other hand, the transparent electrode on the TFT pixel array is formed by patterning the film using wet-chemical etching techniques. Therefore, as the first stage of transparent ZnO electrode development, the GZO films were applied as only the transparent electrode on the RGB color filter in an LCD. In this case, the conventional ITO electrode was used on the TFT pixel array. Concurrently, a technique to form the fine-line patterns of the transparent conductive ZnO film was developed using wet-chemical etching.

4.2 Heat resistance against thermal processing during LCD fabrication

Figure 9 should be referred to again for discussion regarding the heat resistance of GZO films, especially with regards to the behavior of 100 nm thick GZO films because this thickness is close to that used for transparent electrodes in LCDs. During the first heating (step (1)) in the heating cycle test, the compressive residual stress started to reduce suddenly at a specific temperature. The temperature range in which a detectable reduction in the compressive stress occurred in each type of film formed by rf+dc MS, dc MS and RPD was 200-250, 250-300 and 350-400 °C, respectively.

The cause of the decrease in the residual stress with heating to higher than the critical temperature was analyzed using thermal desorption spectrometry (TDS; EMD-WA1000S/W, ESCO Co., Ltd.). The dependence of the amount of Zn mass fragment in the TDS mass spectra on the temperature had the highest correlation with stress for various materials subliming from each GZO film, as shown in Fig. 11(a) (Yamamoto. N. et al., 2008). The temperature at which an observable change in the amount of Zn in the three film types due to volatilization was at 200-250, 250-300 and 300-400 °C, respectively (indicated with arrows). Therefore, it was concluded that the volatilization of Zn from the films at these temperatures during step 1 in the heat-cycle test caused the decrease in the compressive residual stress. The correlation indicates that shrinkage of the film volume accompanied the volatilization of Zn, which resulted in a reverse of the temperature-dependence of the residual stress from increasing compressive stress toward tensile stress.

The order among the critical temperatures at which the change of residual stress and the amount of volatilized Zn began to become significant for the three film types has a good correlation with the order among the lengths of the lattice constant or the wurtzite cell volume as shown in Fig. 4. Longer distances between the atoms in the wurtzite structure is likely to cause weakening of the atomic binding forces, which results in lowering of the heat-resistance of the material.

The heat-resistant properties of the three film types derived from these experimental results were in following order: rf+dc MS < dc MS < RPD. The order of the heat-resistance with respect to the electrical characteristics was exactly the same as that with respect to Zn volatilization and the residual stress. The change in the resistivity, carrier concentration and carrier mobility caused by annealing (heat cycle testing) are compared for films formed by rf+dc MS and RPD in Fig. 11(b). The critical temperatures estimated from the electrical characteristics for the three film types were 200-250 °C (rf+dc MS) < 250-300 °C (dc MS) < 350-400 °C (RPD). This order corresponded exactly with the release of compressive residual stress and Zn volatilization in step (1) during the heat-cycle testing (Yamamoto, N. te al 2010).

Therefore, the films formed by dc MS and RPD have heat resistance properties that are suitable for use as an ITO substitute material for optically transparent electrodes in LCDs. In the case of the film formed by rf+dc MS, the heat resistance characteristics were on the borderline for LCD application. It would be necessary to improve the properties of the rf+dc MS film by some process.

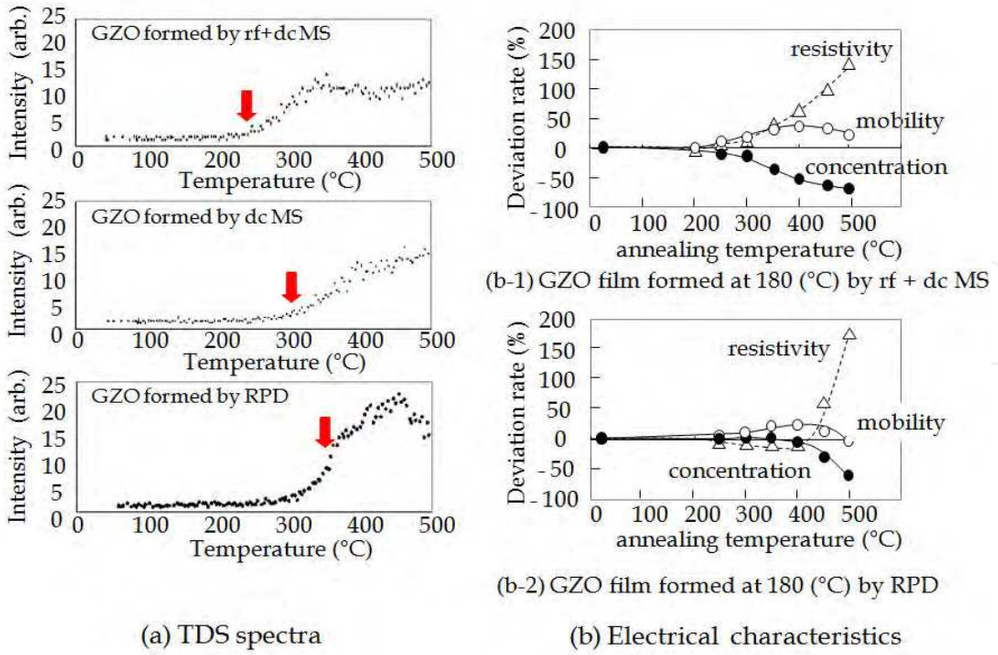

Fig. 11. (a) Comparison of TDS mass spectra for the volatilization of Zn plotted as a function of temperature for 100 nm thick GZO films formed by rf+dc MS, dc MS and RPD at 180 °C. (b) Degradation rates of resistivities, carrier concentrations and carrier mobilities in the films formed by rf+dc MS and RPD at 180 °C as a function of temperature when annealed in flowing Ar (Yamamoto, N. et al., 2010).

4.3 Fabrication of LCDs with transparent ZnO electrode

As the first stage of transparent ZnO electrode development, the GZO electrodes were only applied on the RGB color filter for the manufacture of the LCDs. Conventional ITO films were used as the electrode on the TFT pixel arrays in the LCDs. Among the three film types, the films formed by RPD have the best suited characteristics, such as low electrical resistance and high heat-resistance. However, the current RPD system is not in the usable field for the large size motherglass (1500×1800 mm², 2160×2400 mm² and 2850×3050 mm²) used in the production lines of large size LCD TVs, such 6G (generation), 8G and 10G. Therefore, the conventional dc MS technique, which is used for the formation of ITO transparent electrodes used in commercially available LCDs, was used for the fabrication of LCDs with the GZO electrodes on RGB color filters.

150 nm thick transparent GZO films were formed on the RGB color filters at 150 °C using dc MS. The LCDs were fabricated without change to the process flow, except for the GZO deposition. The fabrication process flow is generally kept an industrial secret. Therefore, the order of the most basic process steps for manufacturing the LCDs are shown as a reference in Fig. 12 (Yamamoto, N. et al., 2010).

The fabrication of the RGB color filter side module and the TFT pixel array side module were carried out separately from each other. After the fabrication reached the final step in each side-module process flow, the two side modules are combined with each other. Consequently, the liquid crystal material is poured into the gap between both substrate sides. LCD fabrication is accomplished through hinging the bezel and attaching various

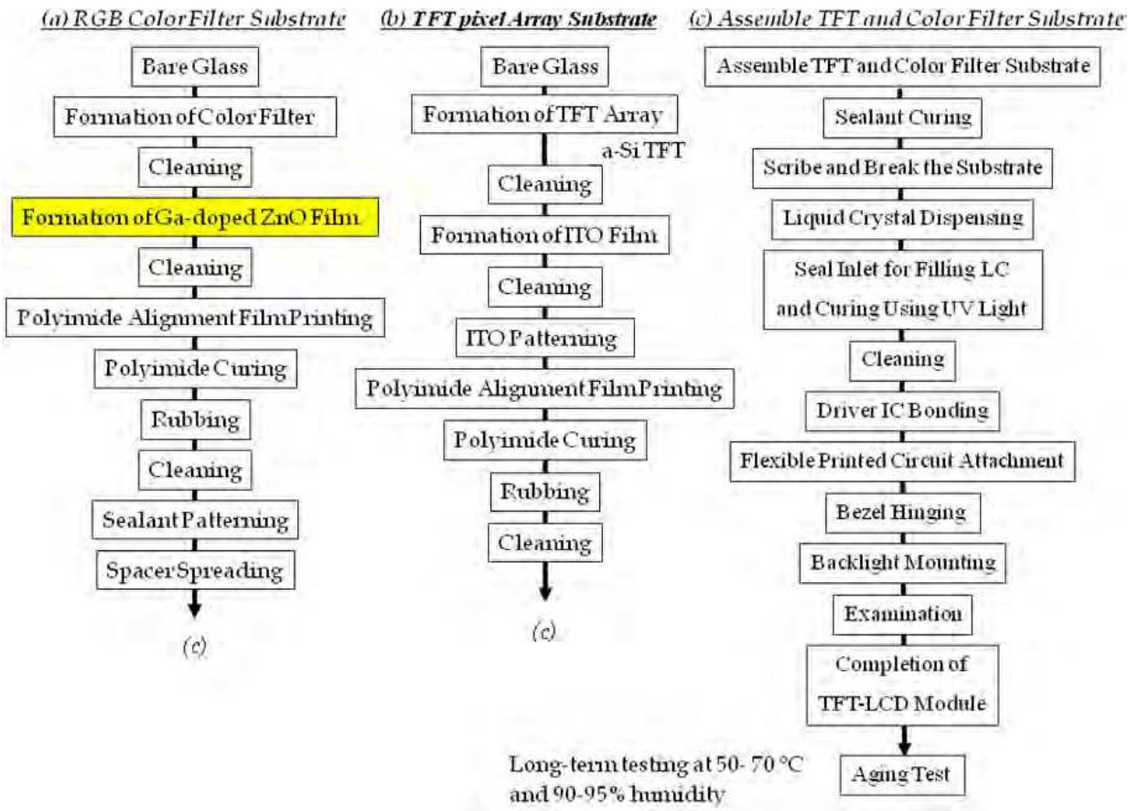

Fig. 12. Basic process flow for manufacture of an LCD with GZO on the RGB color filters.

controlling circuits. Finally the completed LCDs are tested for long term at 50-70 °C in a high humidity (90-95%) environment.

Figure 13 shows the typical display of 3 inch size LCDs and the motherglass before cutting each 3 inch panel part (Yamamoto, N. et al., 2010). The production procedure and process conditions were the same as those for commercially available TFT-LCDs with conventional ITO transparent electrodes, except for the processing step for the formation of transparent conductive GZO films.

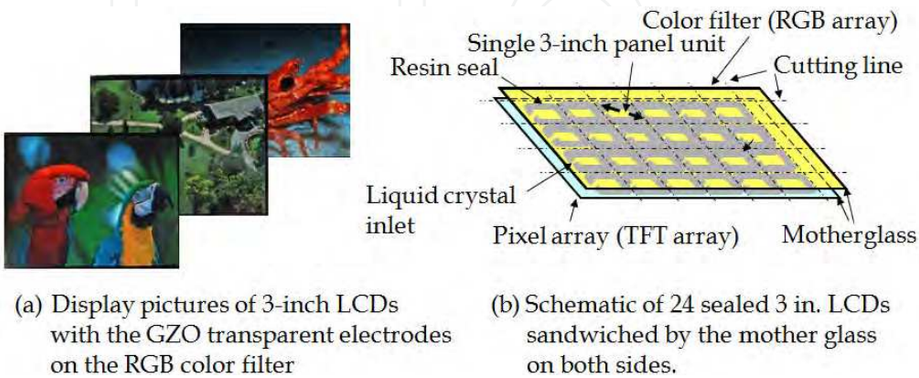

(a) Display pictures of 3-inch LCDs with the GZO transparent electrodes on the RGB color filter

(b) Schematic of 24 sealed 3 in. LCDs sandwiched by the mother glass on both sides.

Fig. 13. (a) Display pictures of 3 inch LCDs with transparent GZO electrodes on the RGB color filters. (b) Schematic of 24 sealed 3 inch LCD sandwiched by the motherglass on both sides.

The displays of 20 inch size LCD TVs with GZO transparent electrodes on the RGB color filters are compared with those of commercially available LCD TVs with ITO electrodes in Fig. 14 (Yamamoto, N. et al., 2011a & 2011c).

Fig. 14. Comparison of the display pictures between 20 inch LCD TVs with GZO and ITO electrodes on the RGB color filter.

The various display properties, such as the contrast ratio of the module, and the chromaticity diagram characteristics, of the LCD TVs with the GZO electrodes were equivalent to those of the LCD TVs with conventional ITO electrodes. The average visible light transmittance of the TV module with the GZO transparent electrode exceeded that of the conventional TV modules with ITO electrodes by 4–5%. These superior characteristics of the GZO module were confirmed by the experimentally measured transmittance of the GZO film in the short wavelength (blue) region of visible light, which exceeded that of polycrystalline and amorphous ITO films (Fig. 8).

The major difference between the 3 inch size LCDs and the 20 inch LCD TVs are the spacers set at the inter-gaps between both side modules. Bead type spacers are distributed between the modules to form a space to inject the liquid crystal, as shown in Fig. 13(b). In the case of the 20 inch LCD TVs, column (rib) type spacers were formed on the plates of the RGB color filters using a conventional photolithography patterning technique. The process steps and the detailed flow for the manufacture of LCD TVs does deviate from that presented in Fig. 12; however, this is proprietary knowledge and the intellectual property of each company.

The display performance of the completed 3 inch LCDs and the 20 inch LCD TVs did not degrade even after long-term operating tests for over 1000 h (on gong) at 50-65 °C in a high humidity (90-95%) environment. Prior to the long-term operation testing, there was some concern regarding degradation of the display performance due to the high humidity environment because the resistance and transmittance of the transparent ZnO film deteriorates under high humidity (Nakagawa, et al., 2009). However, the long-term operation testing results for the LCDs confirmed that transparent ZnO electrodes sealed in the modules of LCDs were not affected by the external environment.

5. Formation of transparent ZnO electrodes with fine-line patterns on TFT pixel arrays

Transparent films formed on the TFT pixel array must be finely patterned using wet-chemical etching techniques. GZO is amphoteric and has low resistance to such agents; therefore, there are no reports on the formation of transparent ZnO patterns with line-widths finer than approximately 10 μm. Thus, the fine-patterning of GZO thin films by wet-chemical etching is a significant developmental challenge.

Fine-patterns of transparent conductive ZnO films were formed by the process flow shown in Fig. 15 (Yamamoto, N. et al., 2011a; 2011b & 2011c). At first, a positive-type novolac-photoresist layer was formed on a transparent conductive ZnO film using a spin-coating applicator for the formation of fine-patterned films. A contact aligner (UV-light exposure system) was used to print the designed mask patterns onto the photoresist layer. The UV-exposed parts in the photoresist layer were removed with a photoresist-developer containing tetramethyl ammonium hydroxide (TMAH, $(CH_3)_4NOH$). The unexposed parts remained as photoresist patterns. Patterning of the GZO films was conducted using a wet-chemical etching technique with organic-acidic etchants; carboxylic acid agents with the photoresist-patterns as the etching mask. The patterning-mask photoresist remaining on the ZnO material patterns was subsequently removed using a photoresist-stripper containing an amine (ELM-R10-F22, produced by Mitsubishi Gas Chemical (MGC) Co., Inc.). The key to realize fine-patterns with widths of a few micrometers is fulfilled by the following three requirements. (1) Development or choice of a suitable developer for the photoresist, i.e., alkaline solution. An aqueous solution prepared by the addition of TMAH to deionized pure water was used as the developer. (2) Development or choice of an acidic solution (etchant) for wet-etching (patterning) of the transparent conductive ZnO films. Solutions based on organic acids and inorganic acid with different pH values were prepared in this work. (3) Optimization of the photolithography and etching processes for GZO films.

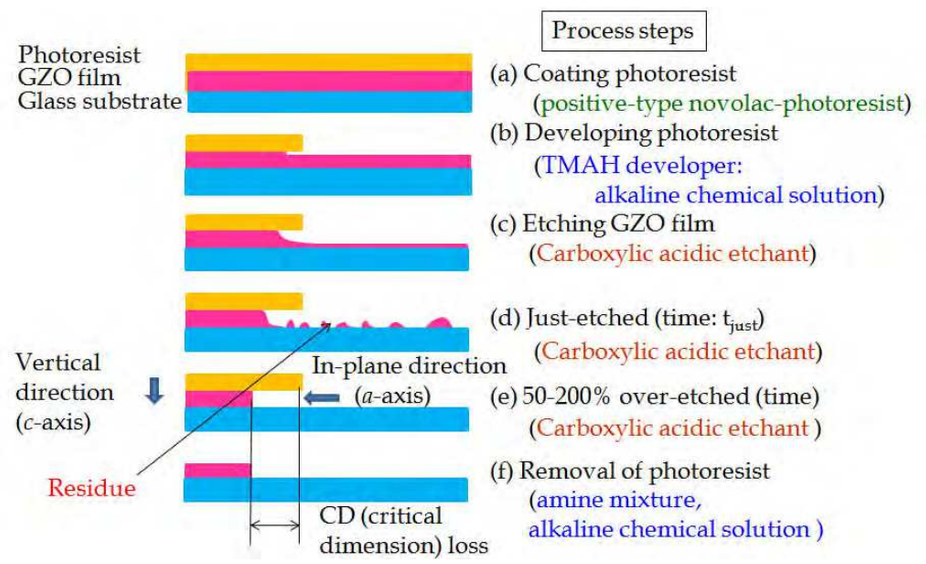

Fig. 15. Process flow for patterning GZO films using wet-chemical etching techniques

The technology for fabricating fine-patterns of transparent conductive ZnO films developed in this work is summarized as follows. The key factors are (1) the development or selection

of appropriate chemical agents, and (2) the determination of an appropriate pH range for each agent (Yamamoto, N. et al., 2011a; 2011b & 2011c).

1. Alkaline chemicals for photolithography process
   a. Developer: TMAH aqueous solution pH: 12.0-13.0
   b. Stripper: Amine chemical solution pH: 11.0-12.0
   (ELM-R10-F22, MGC Inc.)
2. Acidic agent for wet-chemical etching (patterning) pH: 5.5-6.8
   a. Organic acidic etchants (carboxylic acid series) prepared by MGC Inc.
   (Chemical composition: nondisclosur. Not for sale at the present stage)
   b. Inorgabic acidic etchants prepared by Naoki Yamamoto
3. Optimization and control of conditions related to lithography process (UV light exposure, baking of photoresist) and etching process (temperature of etchant, rinsing and drying after etching)

Fine-patterns with line and space widths of a few micrometers were successfully formed using this technology, as shown in the optical micrographs in Fig. 16 (Yamamoto, N. et al., 2011a; 2011b & 2011c).

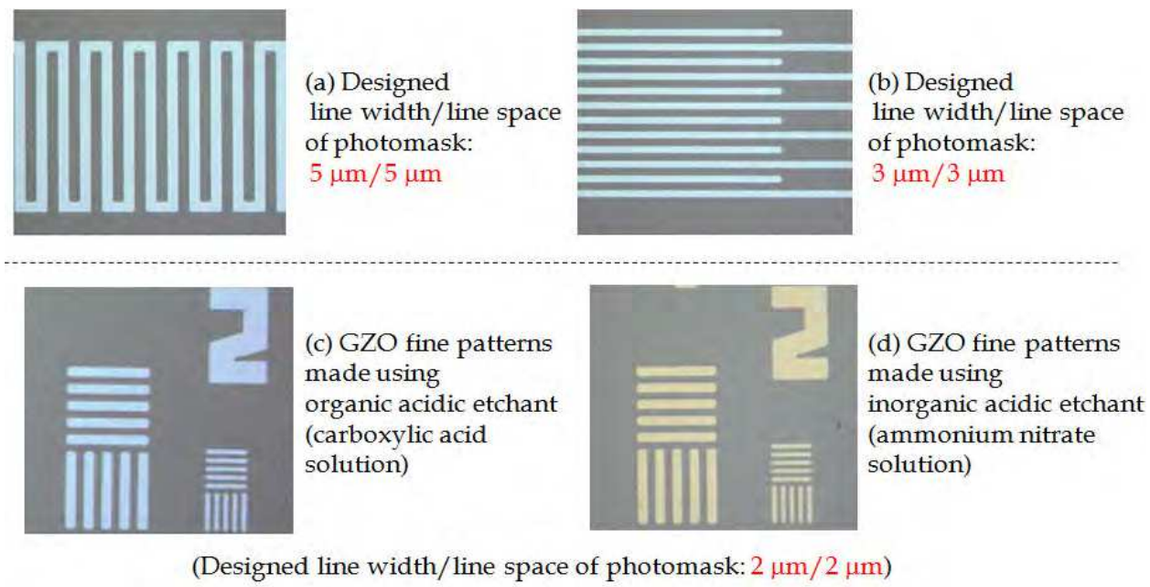

Fig. 16. Typical GZO patterns formed using a weakly acidic etchant (pH 5.5 – 6.8).

Micrographs (a) and (b) show typical meander patterns with line and space widths of 5 μm and comb-like line and space widths of 3 μm, respectively.

Figure 16(c) and (d) shows dense 2 μm line and space patterns of 120 nm- and 150nm- thick GZO film formed successfully using the developed wet-chemical etching technique.

It should be noted here that the patterns shown in Fig. 16 had smooth edges and no residues were observed on the glass substrates after etching of the GZO films. In addition, the 2 μm width line patterns of the GZO film are comparable to the narrowest ITO transparent electrodes formed by wet-etching techniques using leading-edge proximity exposure systems available in commercial LCD production lines.

6. Summary

GZO and AZO films are considered to be the most suitable conductive ZnO films for the current purpose of LCD fabrication. Particular focus was made on the GZO films, because the resistivities of GZO films are lower than those of AZO films.

GZO films have the wurtzite structure as with ZnO films. The resistivity of the GZO films reached approximately 2.4 μΩm, which is in the range of 1.7–3.8 μΩm reported for ITO films formed at temperatures lower than 250 °C.

Conductive ZnO films are amphoteric and are therefore susceptible to acidic and alkaline environments. Therefore, the most important issue for the development of transparent GZO electrodes for LCDs is the development of wet-chemical etching techniques to form fine-patterns with widths of a few micrometers.

The fabrication of LCDs includes process steps that require heating up at 200-250 °C. The thermal resistance of GZO films was investigated from the residual stresses behavior of the films and the volatilization of Zn in the films during heat-cycle testing between room temperature and 500 °C. During the first heating step, the critical temperature where significant Zn volatilization from the GZO film begins coincided with the temperature where significant changes begin to appear in the residual stress and electrical characteristics, that is, resistivity, carrier mobility and carrier concentration. The relationship of these changes with the volatilization of Zn caused by heating the films was clarified. The temperature at which significant change occurs is the critical temperature of the GZO film. The critical temperature was dependent on the method of film formation as follows. The critical temperatures of the films were in the order of 250 °C (rf+dc MS film) < 300 °C (dc MS film) < 400 °C (RPD film). Films formed using dc MS and RPD would therefore be resistant to the thermal process steps conducted at a maximum temperature of 250 °C for the manufacture of LCD panels (TV sets). The transmittance of the GZO film exceeded that of the conventional ITO electrode by ca. 2-7% in the short wavelength region of visible light. As the first development stage of the transparent ZnO electrode, ca. 150 nm thick GZO films were used as only the transparent electrodes on the RGB color filters in 3 inch LCDs and 20 inch LCD TVs. Conventional ITO electrodes were used as the transparent electrodes on the TFT pixel arrays. The initial display performance of both the 3 inch LCDs and the 20 inch LCD TVs was maintained even after long-term operation testing (>2000 h) at 50-65 °C in a high humidity (90-95%) environment.

A wet-chemical etching technique was developed concurrently for the formation of fine-line dense patterns with widths of a few micrometer using the amphoteric GZO films as the 2nd stage of transparent ZnO electrode development. This involved (1) development or selection of appropriate alkaline chemicals for photolithographic processing, (2) development of acidic chemicals for the etching of transparent ZnO films, and (3) optimization of the photolithography and etching processes. The suitable pH range of each chemical agent was determined experimentally, and included the following: (1) TMAH photoresist-developer: pH 12.0–13.2, (2) an etchant for patterning the transparent ZnO film: pH 5.1-6.8, and (3) photoresist remover (stripper): pH 11.0–12.0. Fine line dense patterns with 2 μm line/2 μm space widths were successfully fabricated from 50–150 nm GZO films using these selected reagents and the developed technique. AZO fine-line patterns with the same widths could be also formed using the pattering techniques, because the CD loss (the critical dimension loss is defined as the distance encroached in the ZnO conductive films by acidic etchant from the edge of the patterns under the photoresist layer. reffer Fig.15) dependency rates of AZO films on the over-etched times processed using the acidic etchant were the same as those of the GZO films.

7. Future perspective of transparent ZnO electrode technology

It is expected that LCD TVs manufactured in near future will have the transparent ITO electrodes replaced with transparent ZnO electrodes. Furthermore, the successful development of fine-patterning technology for transparent ZnO films should realize the application of transparent ZnO electrodes to not only LCD TVs that are operated by the VA (vertical alignment) method, but also LCD TVs driven by the IPS (in-plane switching) method. In addition, it is expected that this fine-patterning technology will enable the application of transparent ZnO electrodes to not only LCDs, but also organic LEDs (OLEDs), touch panels LEDs and solar batteries. This technology may also contribute to the development of discrete electronic devices and integrated circuits consisting of ZnO or derivative semiconductors.

8. Acknowledgement

We would like to thank Mr. Ujihara, A., Dr. Ito, T. and co-researchers of Geomatec Co., Ltd. for preparation of the GZO films using a magnetron sputtering system, Mr. Maruyama, T. and co-researchers at Mitsubishi Gas Chemical Co., Inc. for preparation of the chemicals for patterning the GZO films, and Mr. Hokari, H. of Ortus Technology Co., Ltd., for fabrication of the 3 inch LCD panels. We are also grateful to Mr. Morisawa, K. and Mr. Osone, S. of Kochi university of Technology for their support, which aided in the development of the technique for froming the fine-patterns of the ZnO transparent films.
This work was made possible by grants for the Development of Indium Substitute Materials for a Transparent Conducting Electrode in the Rare Metal Substituted Materials Development Project from the Ministry of Economy, Trade and Industry and the New Energy and Industrial Technology Development Organization of Japan.

9. References

Dong, B.-Z.; Fang, G.-J.; Wang,, J.-F.; Guan, W.-J.; & Xing-Zhong Zhao (2007), Effect of thickness on structural, electrical, and optical properties of ZnO: Al films deposited by pulsed laser deposition, *Journal of Applied Physics*, Vol. 101, 033713-1 - 033713-7, ISSN: 0021-8979.

Homma, S.; Miyamoto, A.; Sakamoto, S.; Kishi, K.; Motoi, N. & Yoshimura, K. (2005), Pulmonary fibrosis in an individual occupationally exposed to inhaled indium-tin oxide, Europian *Recipiratory Journal*, Vol. 25, No. 1, pp. 200–204, ISSN: 0903-1936.

Jin, Z. C.; Hamberg, I. & Granqvist, C. G. (1988), Optical properties of sputter-deposited ZnO:Al thin films, *Journal of Applied Physics*, Vol. 64, No. 10, pp. 5117-5131, doi:10.1063/1.342419, ISSN: 0021-8979.

Kempthorne, D. & Myers, M. D. (January 12, 2007), *Mineral Commodity Summaries 2007*, United States Government Printing Office, pp. 78-79. prepared by Carlin, J. F. Jr. U.S. Geological Survey, ISBN-10: 0160778956, ISBN-13: 978-0160778957. http://minerals.usgs.gov/minerals/pubs/mcs/2007/mcs2007.pdf

Moss, T. S., (1980), Theory of intensity dependence of refractive index, *Physica Status Solidi (b)*, Vol. 101, No. 2, pp. 555-561, ISSN: 0370-1972

Nakagawara, O.; Kishimoto, Y.; Seto, H.; Koshido, Y.; Yoshino, Y.; Makino, T. (2009), Moisture-resistant ZnO transparent conductive films with Ga heavy doping, *Applied Physics Letters*, Vol.89, No.9, pp. 091904 - 091904-3, ISSN: 0003-6951.

Ofuji, M.; Inaba, K.; Omote, K.; Hoshi, H.; Takanishi, Y.; Ishikawa, K. & Takezoe, H. (2002), Grazing incidence in-plane X-ray diffraction study on oriented copper phthalocyanine thin films", Japanese Journal of Applied Physics, Part 1, vol. 41, No. 8, pp. 5467–5471, ISSN: 0021- 4922.

Shin, S. H.; Shin, J. H.; Park, K. J.; Ishida, O. & Kim, H. H. (1999), Low resistivity indium tin oxide films deposited by unbalanced DC magnetron sputtering, *Thin Solid Films*, Vol. 341, issues 1-2, pp. 225 – 229, ISSN: 0040-6090.

Thornton, J. A. & Hoffman, D. W. (1977), Internal stresses in titanium, nickel, molybdenum, and tantalum films deposited by cylindrical magnetron sputtering, *Journal of vacuum science and technology*, Vol. 14, pp. 164- 168, ISSN 0022-5355.

Wakeham, S. J.; Thwaites,M. J.; Holton, B. W.; Tsakonas, C.; Cranton, W. M; Koutsogeorgis, D. C. & R. Ranson (2009), Low temperature remote plasma sputtering of indium tin oxide for flexible display applications, *Thin Solid Films* doi:10.1016/j.tsf.2009.04.072, ISSN: 0040-6090.

Wortman J. J. & Evans, R. A. (1965), Young's Modulus, Shear Modulus, and Poisson's Ratio in Silicon and Germanium, *Japanese Journal of Applied Physics*, Vol. 36, pp. 153 – 156, doi:10.1063/1.1713863, ISSN: 0021-8979

Yamada, T.; Miyake, A.; Kishimoto, S.; Makino, H.; Yamamoto, N. & Yamamoto, T. (2007) Low resistivity Ga-doped ZnO thin films of less than 100 nm thickness prepared by ion plating with direct current arc discharge, *Applied Physics Letters*, Vol. 91, 051915, doi:10.1063/1.2767213 (*3 pages*). ISSN : 0003-6951.

Yamamoto, N.; Kume, K.; Iwata, S.; Yagi, K. & Kobayashi, N. (1986), Fabrication of highly reliable tungsten gate MOS VLSI's, *Journal of the Electrochemical Society*, Vol. 133, No.2, pp. 401-407, ISSN: 0013-4651.

Yamamoto, N.; Yamada, T.; Miyake, A.; Makino, H.; Kishimoto, S. & Yamamoto, T. (2008), Reletionship between residual stress and crystallographic structure in Ga-doped ZnO film, *Journal of the Electrochemical Society*, Vol. 155, No. 9, pp. J221-J225, ISSN: 0013-4651.

Yamamoto, N.; Makino, H.; Yamada, T.; Hirashima, Y.; Iwaoka, H.; Ito, T.; Ujihara, A.; Hokari, H.; Morita, H. & Yamamotoa, T. (2010), Heat resistance of Ga-doped ZnO thin films for application as transparent electrodes in liquid crystal displays, *Journal of the Electrochemical Society*, Vol. 157, No. 2, pp. J13-J20, ISSN: 0013-4651.

Yamamoto, N.; Makino, H.; Osone, S.; Ujihara, A.; Ito, T.; Hokari, H.; Maruyama, T. & Yamamoto, T. (2011a), Development of Ga-doped ZnO transparent electrodes for liquid crystal display panels, , *Thin Solid Films*, doi: 10.1016/j.tsf.2011.04.067, Article in press, ISSN: 0040-6090.

Yamamoto, N.; Makino, H.; Sato, Y. & Yamamoto, T, (2011b), Controlled formation of ZnO fine-pattern transparent electrodes by wet-chemical etching, ECS Transactions, Vol. 35, Issue 8, pp. 165 – 172, ISSN: 1938-5862.

Yamamoto, N.; Makino, H.; Sato, Y. & Yamamoto, T (2011c), Development of Ga–doped ZnO Transparent Electrodes as Alternatives for ITO Electrodes in Liquid Crystal Displays, the *SID 2011 digest of technical papers*, pp. 1375-1378, ISSN: 0097-966X.

Yamamoto, T.; Yamada, T.; Miyake, A.; Makino, H. & Yamamoto, N. (2008), Ga-doped zinc oxide: An attractive potential substitute for ITO, large-area coating, and control of electrical and optical properties on glass and polymer substrates, *Journal of the Society for Information Display*, Vol. 16/7, pp. 713-719, ISSN: 1071-0922.

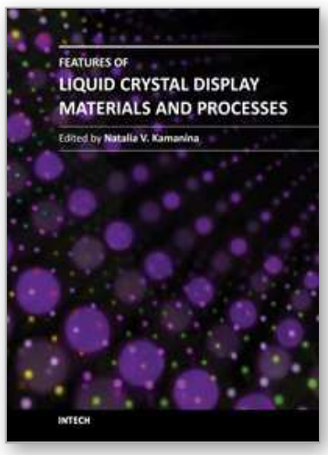

Features of Liquid Crystal Display Materials and Processes

Edited by Dr. Natalia Kamanina

ISBN 978-953-307-899-1
Hard cover, 210 pages
Publisher InTech
Published online 30, November, 2011
Published in print edition November, 2011

Following the targeted word direction of Opto- and Nanoelectronics, the field of science and technology related to the development of new display technology and organic materials based on liquid crystals ones is meeting the task of replacing volume inorganic electro-optical matrices and devices. An important way in this direction is the study of promising photorefractive materials, conducting coatings, alignment layers, as well as electric schemes that allow the control of liquid crystal mesophase with good advantage. This book includes advanced and revised contributions and covers theoretical modeling for optoelectronics and nonlinear optics, as well as includes experimental methods, new schemes, new approach and explanation which extends the display technology for laser, semiconductor device technology, medicine, biotechnology, etc. The advanced idea, approach, and information described here will be fruitful for the readers to find a sustainable solution in a fundamental study and in the industry.

INTECH
open science | open minds

InTech Europe
University Campus STeP Ri
Slavka Krautzeka 83/A
51000 Rijeka, Croatia
Phone: +385 (51) 770 447
Fax: +385 (51) 686 166
www.intechopen.com

InTech China
Unit 405, Office Block, Hotel Equatorial Shanghai
No.65, Yan An Road (West), Shanghai, 200040, China
中国上海市延安西路65号上海国际贵都大饭店办公楼405单元
Phone: +86-21-62489820
Fax: +86-21-62489821

IntechOpen